ELSEVIER

Biochimica et Biophysica Acta 1235 (1995) 169–177

BBA Biochimica et Biophysica Acta

Solution structure determination by NMR spectroscopy of a synthetic peptide corresponding to a putative amphipathic α-helix of spiralin: resonance assignment, distance geometry and simulated annealing ☆

Arnaud Bondon [a,*], Patrick Berthault [b], Isabelle Segalas [b], Bruno Perly [b], Henri Wróblewski [c]

[a] *Laboratoire de Chimie Organometallique et Biologique, URA CNRS 415, Université de Rennes I, 35042 Rennes Cedex, France*
[b] *DRECAM / SCM, CE Saclay, 91191 Gif sur Yvette, France*
[c] *Département 'Membranes et Osmoregulation', URA CNRS 256, Université de Rennes I, 35042 Rennes Cedex, France*

Received 8 August 1994; accepted 24 November 1994

Abstract

Spiralin is the major protein of the plasma membrane of several spiroplasmas. Neither the function of this protein nor the crystallographic structure is known. Analysis of the primary structure of spiralin from *Spiroplasma melliferum* BC3 suggests the presence of an amphipathic peptide in the 143–162 region (Chevalier, C., Saillard, C. and Bové, J.M. (1990) J. Bacteriol. 172, 6090–6097). The structure of a synthetic peptide, H_2N-L-N-A-V-N-T-Y-A-T-L-A-K-A-V-L-D-A-I-Q-N-amide, corresponding to this fragment has been examined by ^{1}H-NMR spectroscopy. This 20 amino acid peptide adopts a random coil structure in solution, but the addition of trifluoroethanol stabilizes a structure exhibiting α-helical character. The ^{1}H-NMR spectrum has been fully assigned in CF_3CD_2OD/H_2O (30:70, v/v) and the three-dimensional structure has been elucidated using NMR-derived distance information. The calculated structures have been obtained by dynamical simulated annealing or distance geometry followed by simulated annealing. Both sets of structures have been energy-minimized using CHARMm potential. The resulting structures are very similar in terms of constraint violations and energies. It is demonstrated that whereas the first three residues exhibit a large flexibility, the remaining sequence is helical.

Keywords: Structure determination; Amphipathic helix; Alpha helix; Spiralin; NMR; Distance geometry; Annealing

1. Introduction

Mollicutes (trivial name, mycoplasmas) are the smallest and the simplest bacteria capable of self-replication. The size of their genome is in the 600–1700 kb range and their cell envelope is made of only the plasma membrane. Hence, mollicutes are among all known living organisms those which best illustrate the concept of the 'minimal cell' [1]. A prominent feature of several mollicutes is the large number of membrane proteins containing covalently bound fatty acids [2]. As these acylated proteins are exposed on the mycoplasma cell surface, it is believed that they play some role in connection with the interactions between mycoplasmas and their milieu which is in most if not in all cases a human, animal or plant host.

More specifically, the plasma membrane of some species of spiroplasmas (helical mollicutes) contains a major 26 kDa polypeptide called spiralin which has previously been purified [3,4] and shown to being acylated, mainly by myristate and palmitate [5]. Though the gene encoding spiralin has been cloned in *Escherichia coli* [6] and sequenced [7,8], the function of this protein is still unknown. Spiralin being unrelated to any protein of known structure and/or function, the determination of its biological function requires to determine its topography and notably to know whether or not it spans the membrane. The two topological models proposed so far suggest that spiralin might be a bitopic protein [5,8]. In the later model, based on secondary structure prediction, a twenty-residue amphipathic α-helix localized within the last third of the sequence has been proposed as the putative transmembrane

☆ Dedicated to Professor Rene Dabard on the occasion of his 64th birthday.

Abbreviations: 1D, one dimensional; 2D, two dimensional; TFE, trifluoroethanol; COSY, correlation spectroscopy; DQF COSY, double quantum filtered correlation spectroscopy; DRCT, double relayed coherence transfer spectroscopy; NOE, nuclear Overhauser enhancement; NOESY, 2D NOE spectroscopy; DG/SA, distance geometry-dynamical simulated annealing; SA, simulated annealing; RMSD, root mean square deviation.

* Corresponding author. Fax: +33 99 281646.

SSDI 0005-2736(94)00286-X

segment of the protein [8]. However, evidence for the presence of a cleavable N-terminal signal sequence [9], suggests that spiralin does not span the lipid bilayer but is, on the contrary, a monotopic membrane protein anchored to the outer face of the bilayer thanks to its acyl chain(s). This model is supported by the fact that the α-helix mentioned above is related to globular protein helixes and contains a B-cell epitope (see the accompanying paper by Brenner et al. [36]).

In order to provide a more accurate description of the conformation, we have investigated by ^{1}H-NMR spectroscopy the solution structure of a synthetic peptide corresponding to the putative amphipathic α helix of *Spiroplasma melliferum* BC3 spiralin. Specifically, this paper describes the ^{1}H-NMR assignment of the peptide dissolved in 30% TFE. The solution structure was performed through a quantitative analysis of the NOE information by distance-geometry or simulated annealing calculations.

2. Materials and methods

2.1. Peptide synthesis

The 143–162 peptide fragment of the spiralin from *Spiroplasma melliferum* BC3 (for numbering see Fig. 1) was prepared using solid-phase peptide synthesis. The detailed description of the synthesis and of the purification is described in the accompanying paper by Brenner et al. [36]. The peptide sequence (H_2N-L-N-A-V-N-T-Y-A-T-L-A-K-A-V-L-D-A-I-Q-N-amide) will be numbered from 1 to 20, in this paper.

2.2. NMR spectroscopy

NMR spectra were recorded at 293 K on either a Bruker AC 300P or a Bruker AM 300WB spectrometer (C.R.M.P.O. Rennes). Some spectra were also recorded at 600 MHz on a Bruker AMX 600 spectrometer. Unless otherwise indicated, the peptide was dissolved in 30% (v/v) TFE-d_3/H_2O (or D_2O) to 2–4 mM (no concentration dependence was observed). Uncorrected pH values were read from a Schott Gerate CG pH meter equipped with an Ingold microcombination electrode. Chemical shifts are referenced to external DSS (4,4-dimethyl-4-silapentane-1-sulfonate) through the residual water resonance. All two-dimensional experiments were recorded in a phase sensitive mode using time-proportional phase incrementation [10]. Typically, 400 to 512 increments were collected with 2 K points. After zero filling in F1, the time domains were multiplied by a phase shifted sine bell function in both dimensions. During the 1.2 s recycle time, the water resonance was saturated by continuous low-power irradiation from the decoupler channel. No substantial difference in the intensity of amide protons was observed when the water resonance was suppressed by a jump and return sequence [11]. Double quantum filtered (DQF) COSY [12,13], double relayed coherence transfer spectroscopy (DRCT) [14,15], NOESY [16] spectra (mixing time of 100 and 200 ms) were acquired at 300 MHz. In order to get accurate integrations of the NOE cross-peaks NOESY spectra (mixing time of 150 and 250 ms, recycle time of 1.7 s) were also performed at 600 MHz.

2.3. Interproton distance constraints

The relative NOE cross-peak volumes have been converted into proton-proton distances. The cross-peak intensities were classified into strong, medium, weak and very weak for which corresponding upper limits were set to 2.5, 3, 4 and 5 Å, respectively. A total of 205 NOE cross-peaks have been collected, among which 84 interresidue dipolar interactions. Neither spin diffusion nor internal motions have been taken into account, only upper limits were used for the distance constraints (error range around 0.2 Å). The lower limit has been set to 1.8 Å which is approximately the sum of the Van der Waals radii. Since no stereospecific assignment has been done, the constraints in prochiral centers, methyl groups and aromatic rings could not be distinguished. The pseudo-atom facilities have therefore been used in these case.

2.4. Dihedral constraints

All $^3J_{HN\text{-}H\alpha}$ coupling constant values for residues 2–20, determined from one-dimensional spectra, have been converted into dihedral information, on phi angles, using a semi-empirical Karplus-type relation [17]. For all the procedures, a square-well shaped of the dihedral restraint term scaled with standard value [18] was applied. Due to the lack of precision of both the Karplus-type relation and the square-well shaped of the dihedral restraint term large error ranges were observed during the minimization.

Fig. 1. Sequence of *Spiroplasma melliferum* BC3 spiralin in one letter code. The sequence is from Chevalier et al. [8] and is modified to take into account the cleavage of a 23-residues signal peptide between alanine^{-1} and cysteine^{+1} [9]. The putative amphipathic α-helix encompasses residues 143–162.

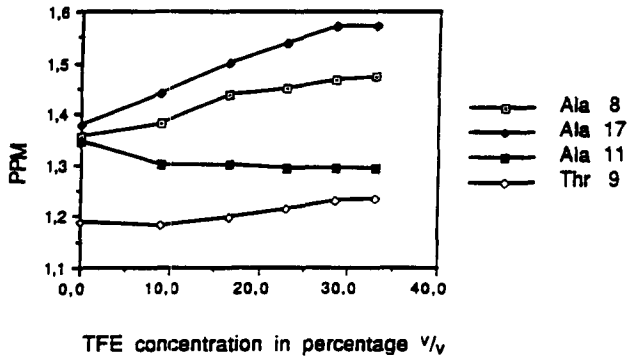

Fig. 2. Plots of the chemical shift of several resonances versus TFE concentration.

2.5. Molecular modeling

Calculations were performed on an IBM RISC System 6000/530 using the X-PLOR 3.0 software package [18]. Visualization was performed using the QUANTA program (Polygen, Waltham, MA). Two different methods were compared together. First, the hybrid distance geometry-dynamical simulated annealing protocol of X-PLOR [19,20] has been used. Second, dynamical simulated annealing has been performed [21]. Both sets of final structures were further energy-minimized with CHARMm parameters set 19 [22]. Comparison of these two methods permits to check their conformational sampling properties as well as their respective performances. For clarity, we will refer to these methods as DG/SA and SA.

2.6. Hybrid distance geometry-simulated annealing

A total of 60 conformations have been generated by sub-structure embedding. These sub-structures were regularized, after embedding, by minimization against an energy term (target function) representing all upper and lower bounds in the bound matrix. The structures were then submitted to simulated annealing. As the first step, the presence of the correct enantiomers were checked by energy discrimination. The following step allowed to generate the missing atoms and regularize the structure, using a short minimization of bonds, repulsive Van der Waals terms, dihedral restraints and NOE energetic constraints. Angle terms were then added to the energy function, and further minimization was performed. Simulated annealing was carried out by a slow introduction of chirality and planarity information and a decrease of the weight of the Van der Waals term in 2 ps of 2000 K annealing (2 fs time step). Cooling to 100 K was achieved over a period of 2 ps, with an increase of the repulsive Van der Waals force

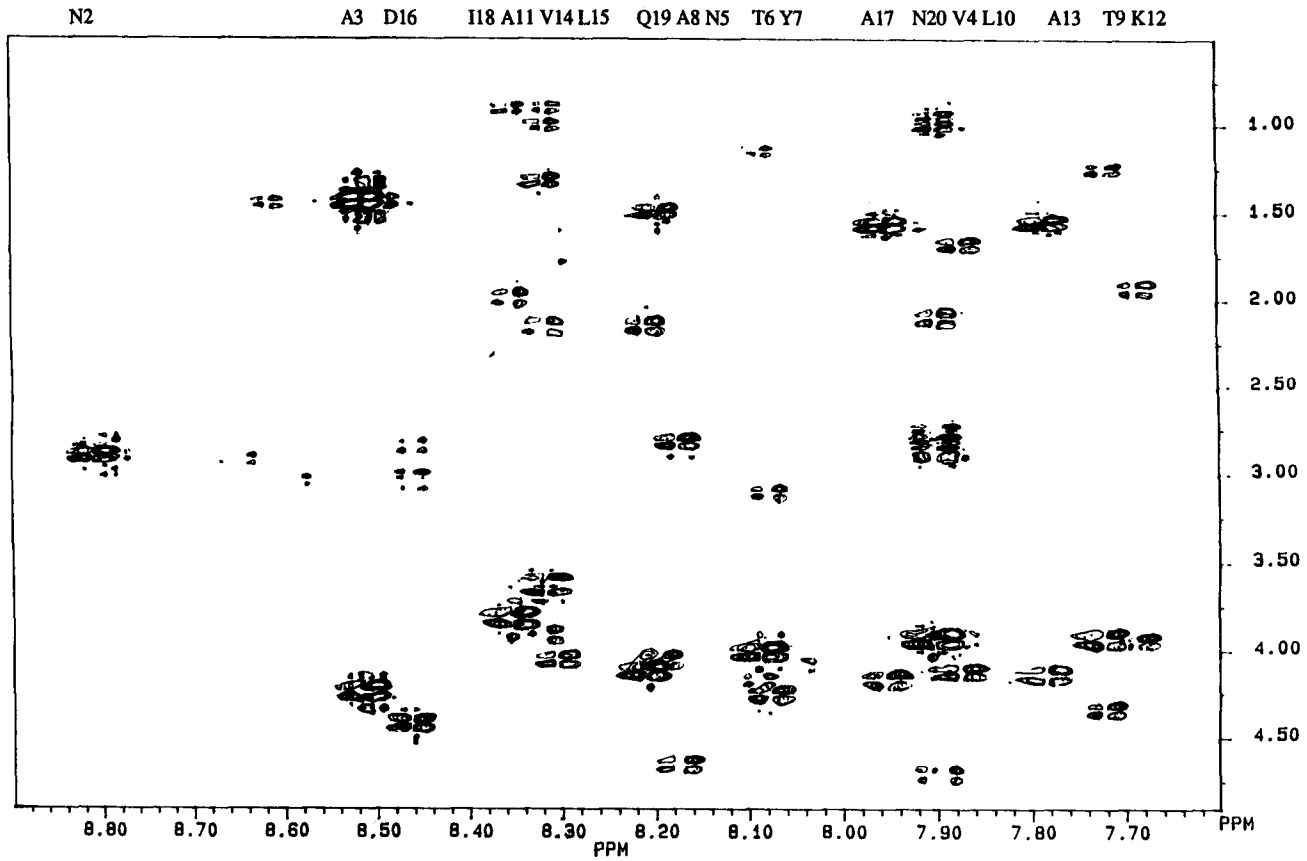

Fig. 3. Portion of DRCT spectrum showing the scalar correlation of the amide protons with the side-chain protons (Hα, Hβ and Hγ). The amide protons are labelled at the top of the 2D map.

constant and a distance constraint force constant set to 50 kcal $Å^{-2}$. Along the entire process, coupling to a progressively decreasing temperature bath was controlled.

2.7. Simulated annealing

60 structures have been generated by 'ab initio' simulated annealing [21]. Starting from an extended conformation, a first phase of 12 ps dynamics with a time step of 2 fs at high temperature (1000 K) was followed by a 6 ps slow cooling to 100 K (using the same time step). Different choices of the initial random number seed, in the high temperature dynamic, resulted in different initial velocities, and thus produced a large variation of the structures. A small weight of the van der Waals repulsive term was used at high temperature in order to allow a large conformational sampling. The variation of the slope of the asymptote in the NOE potential function allowed a progressive fit of the distance constraints. During all this process the distance constraint force was kept to 50 kcal $Å^{-2}$.

2.8. Energy minimization of the structures

Both sets of structures obtained from DG/SA or SA were subjected to further refinement. A 6 ps simulated annealing procedure from 2000 K to 100 K (timestep 3 fs), with smoothing of the Van der Waals repulsions and a square shaped NOE potential ($k_{NOE} = 50$ kcal $Å^{-2}$) was applied. The final structures were analyzed and selected using acceptance criteria on the constraints and the geometry. The structures exhibiting either NOE violations larger than 0.5 Å or dihedral violations larger than 5 degrees have been eliminated. Moreover, two other acceptance criteria relative to the ideal geometry were no RMSD larger than: (i) 0.01 Å for the bond lengths and (ii) 1 degree for the bond angles. The accepted structures have been then energy minimized in 500 steps with full CHARMm force field (parameters set 19) without NOE nor dihedral constraints. A dielectric constant linearly dependent of the interatomic distance has been used with a value of 1.0 at 1 Å.

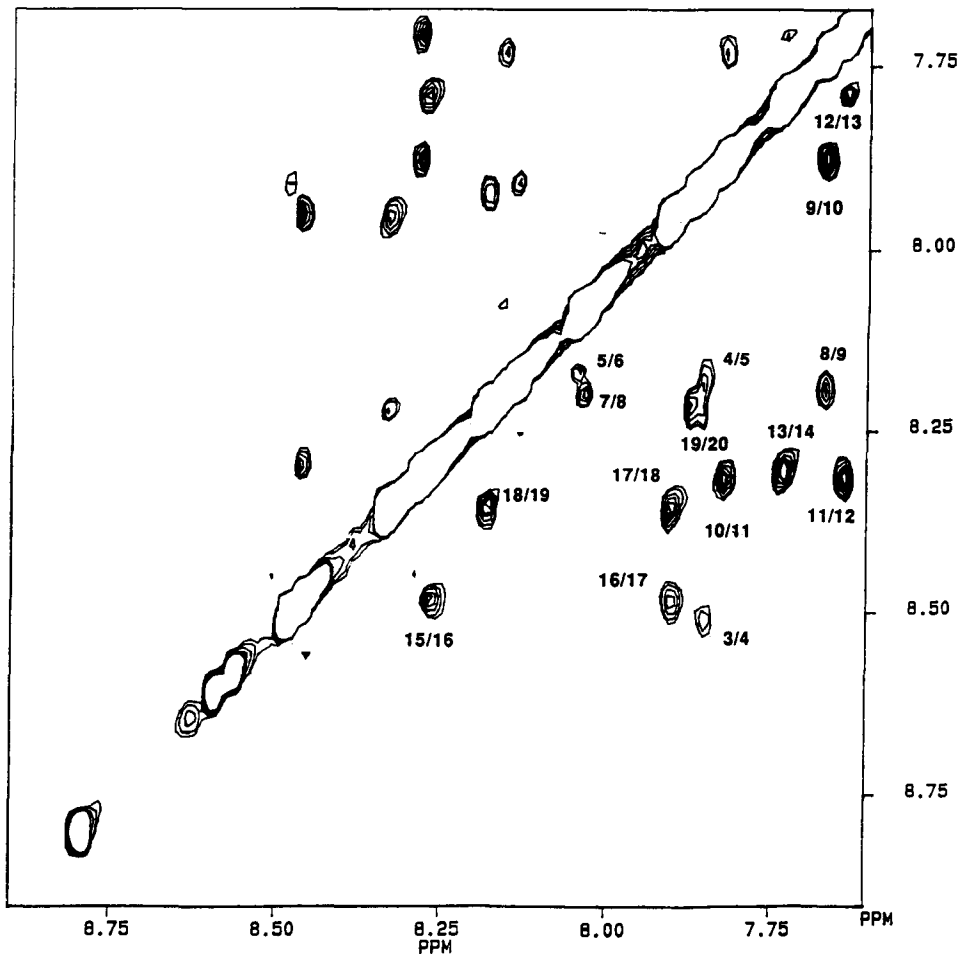

Fig. 4. 600 MHz phase sensitive NOESY spectrum (mixing time 150 ms) of the 143–162 fragment of spiralin showing NH-NH cross-peaks. Interactions involving successive residues are labelled.

Table 1
Assignment of proton resonances of a synthetic peptide corresponding to the 143–162 sequence of *Spiroplasma melliferum* BC3 in 30% TFE/70% H_2O at 293 K, pH 3.3

Residue	NH	CαH	CβH	CγH	Other
Leu-1		4.02	1.72, 1.72	1.66	0.91, 0.91
Asn-2	8.80	4.75	2.92, 2.92		6.78, 7.58
Ala-3	8.52	4.22	1.43		
Val-4	7.89	3.91	2.08	0.93, 0.96	
Asn-5	8.17	4.63	2.80, 2.82		6.77, 7.54
Thr-6	8.08	3.98	4.18	1.13	
Tyr-7	8.07	4.23	3.07, 3.11		7.08, 6.78
Ala-8	8.19	4.05	1.47		
Thr-9	7.73	3.92	4.33	1.23	
Leu-10	7.86	4.10	1.65, 1.65	1.68	0.82, 0.82
Ala-11	8.33	3.90	1.28		
Lys-12	7.68	3.92	1.93, 1.93	1.43, 1.60	1.68, 1.68, 2.99, 2.99
Ala-13	7.78	4.11	1.54		
Val-14	8.32	3.60	2.13	0.88, 0.99	
Leu-15	8.31	4.05	1.57, 1.78	1.79	0.83, 0.83
Asp-16	8.45	4.40	2.83, 3.05		
Ala-17	7.95	4.13	1.55		
Ile-18	8.35	3.82	1.98	1.17, 1.78	0.80 γCH_3 0.88
Gln-19	8.20	4.09	2.14, 2.14	2.35, 2.53	6.58, 7.08
Asn-20-$CONH_2$	7.88	4.67	2.78, 2.85		6.78, 7.58, 7.05, 7.23

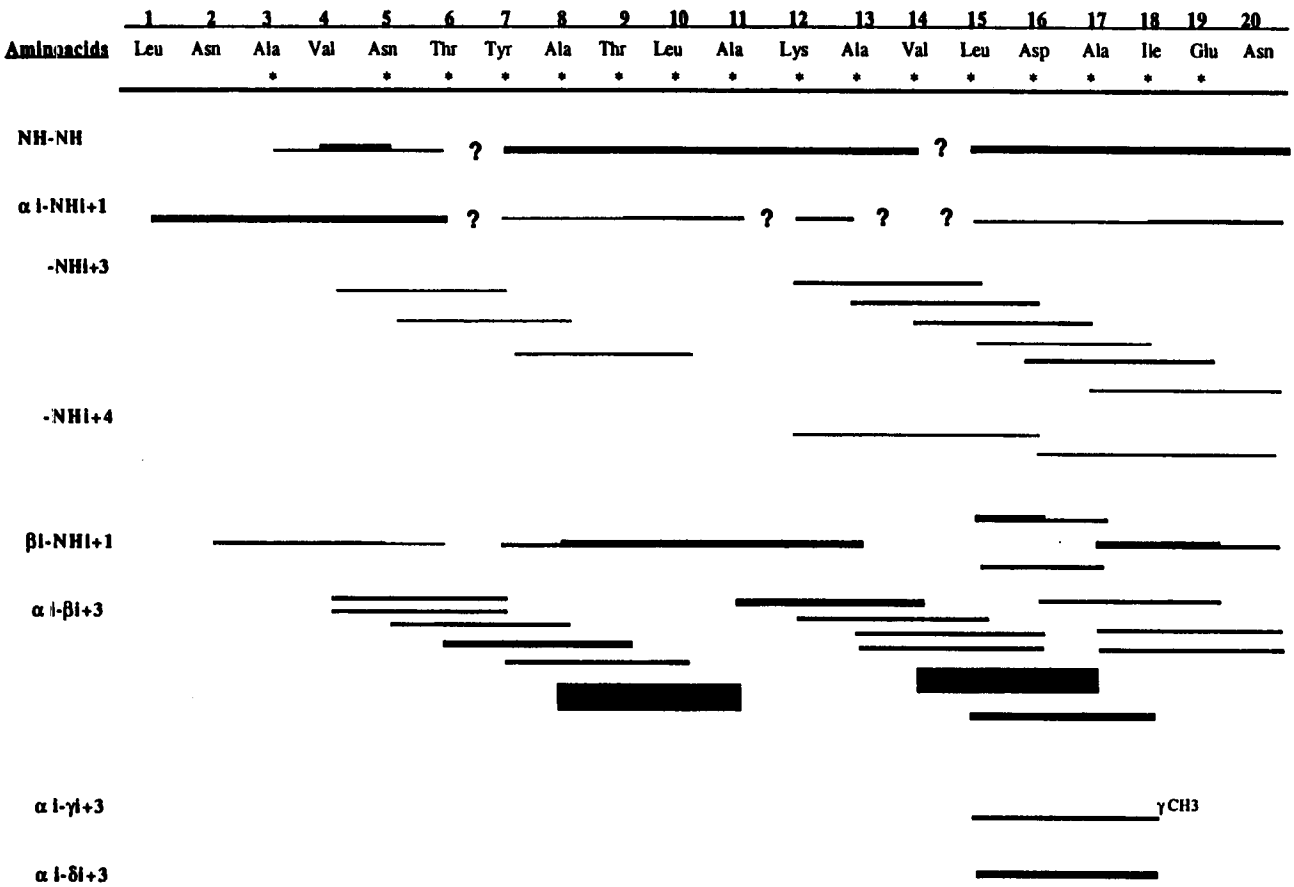

Fig. 5. Summary of the interresidue NOEs observed in the 150 msec NOESY spectrum. The heights of the bars indicate the intensities of the NOEs. Ambiguous sequential cross-peaks because overlapping resonances are indicated by a ?. The asterisks indicate residues for which $^3J_{NH-\alpha H}$ coupling constant is less than 6 Hz.

3. Results

3.1. Influence of TFE on secondary structure

No significant changes were observed in the 1D NMR spectra of the peptide dissolved in pure water, neither at two temperatures (278 K and 293 K) nor in the 2–8 pH range. Conversely, addition of TFE results in large variation of the proton NMR spectrum. Many resonances were shifted with increasing concentration of TFE. In Fig. 2, the chemical shift of selected resonances is plotted against the TFE concentration, at 293 K. The maximum effect of the TFE was clearly reached around 30%. Attempts to determine by NMR the minimal percentage of TFE corresponding to the maximum stabilizing effect, at 278 K, were unsuccessful because of the immediate aggregation of the peptide in 10% TFE. Conversely, at 293 K and 30% TFE, some line broadening of the resonances occurred only after 50 h and the solution finally fully jellified after several days (no clear concentration dependence was observed during this study).

3.2. ^{1}H-NMR resonance assignments

Proton resonance assignments were made, at 293 K and 30% TFE, by standard NMR procedures involving identification of amino acid spin systems and sequential resonance assignment [23]. All 19 amide protons (NH) can be observed on the 1D NMR spectrum (not shown). All but one NH-αH cross-peaks are present in the DQF COSY spectrum (not shown) and in the DRCT spectrum in Fig. 3. The DRCT spectrum also contains the NH-βH and the NH-γH connectivities (Fig. 3). Most of the side-chain resonances could be fully identified from this DRCT spectrum, with the exception of three leucines, one isoleucine and one lysine. The completion of these spin system connectivities was obtained from the DQF COSY of the aliphatic region (not shown).

The sequence specific assignment was achieved from the NOESY spectra using both d_{NN} $(i, i+1)$ and $d_{\alpha N}$ $(i, i+1)$ cross-peaks. Four interruptions in the $d_{\alpha N}$ $(i, i+1)$ sequential connectivities were caused by overlapping resonance of NH or αH signals. With two exceptions, continuous d_{NN} $(i, i+1)$ cross-peaks were identified, in the NOESY spectrum, from the Ala-3 and the Asn-20 (Fig. 4). The two missing cross-peaks correspond to the Thr-6/Tyr-7 and Val-14/Leu-15 connectivities. Fortunately, the presence of only one tyrosine and two valine residues permits, in comparison with the peptide sequence and the spin system identification, to complete the assignment. The complete list of resonance assignments is given in Table 1.

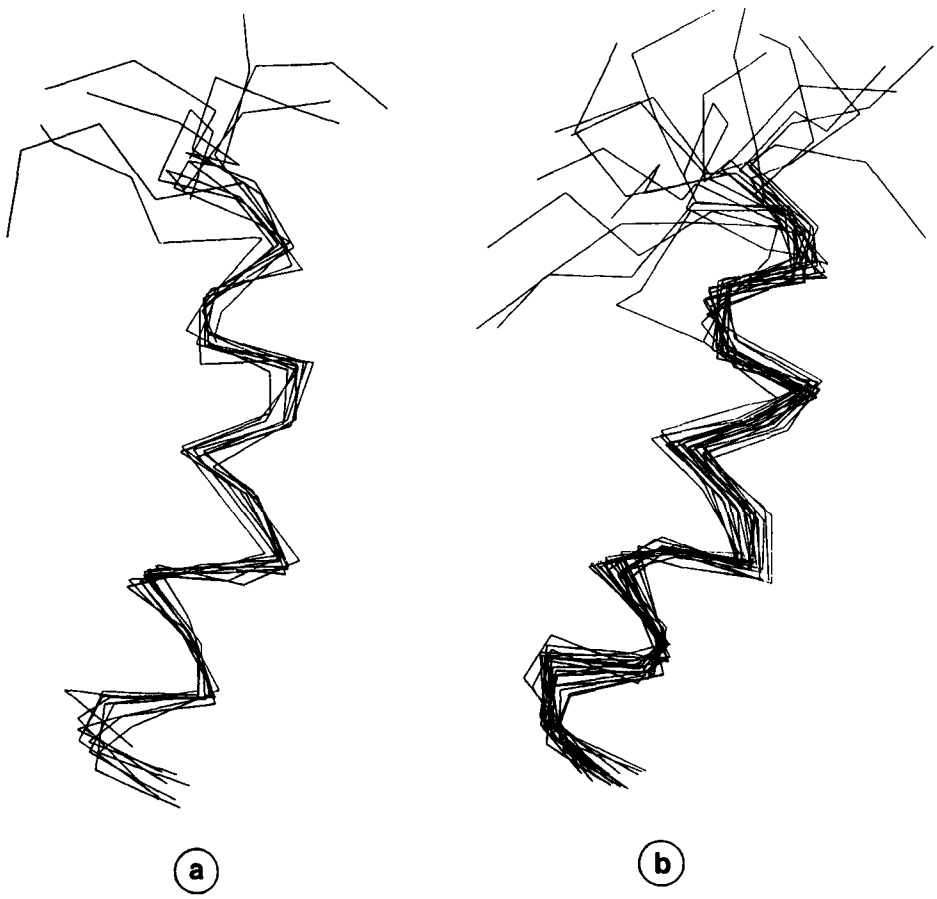

Fig. 6. Superimposition of the backbone atoms of the accepted structures obtained from DG/SA (a), SA (b). The structures are positioned to optimize the match of the backbone atoms of the residues 4 to 20. Only backbone atoms are displayed.

3.3. Identification of the secondary structure

As already pointed out, the addition of TFE induced large changes in the 1D NMR spectra of the peptide. These chemical shift variations are associated with the stabilization of well-defined secondary structure. Analysis of the sequential connectivities and the interresidue cross-peaks might be useful for the distinction between different secondary structure elements [23]. Numerous intense d_{NN} $(i, i+1)$ cross-peaks are indicative of helical secondary structure. Another evidence of an α-helix is associated with the presence of a large number of interresidue connectivities, as summarized in Fig. 5. Despite of overlapping CαH and NH resonances, several $d_{\alpha N}$ $(i, i+3)$ cross-peaks were observed. Also, in the case of the $d_{\alpha\beta}$ $(i, i+3)$ connectivities numerous cross-peaks were identified from Val-4 to Asn-20. In contrast, for the first three residues the absence of $d_{\alpha N}$ $(i, i+3)$, $d_{\alpha\beta}$ $(i, i+3)$ and d_{NN} $(i, i+1)$ cross-peaks, as well as the medium intensity of the $d_{\alpha N}$ $(i, i+1)$ connectivities, indicate that this region is predominantly flexible. The NOESY data indicate that the most stable helix spans from residues 4 to 20.

Further evidence for the helix structure of the peptide can be obtained from the $^3J_{NH\text{-}\alpha H}$ obtained from the 1D NMR spectrum. The dependence of $^3J_{NH\text{-}\alpha H}$ on the torsion angle phi is well documented [23]. However, due to the lack of precision of the Karplus-type relationships and the square-well shape of the dihedral constraint term large error ranges were required. Small coupling constant values are indicative of helical structure. Under the conditions used in the present study, sixteen of the $^3J_{NH\text{-}\alpha H}$ coupling constants are under 6 Hz, in agreement with the preponderant helical conformation of the peptide (Fig. 5).

3.4. Three-dimensional structural determination

Two different approaches, described under Materials and methods, have been used for the structural determination: DG/SA and SA. Two sets of 60 structures, consistent with experimental NOE distance constraints, were generated using these two methods of simulation. After refinement, 9 and 19 structures were accepted for the DG/SA and the SA protocols, respectively. The superimposed structures over the backbone atoms 4–20 are shown in Fig. 6a and b. All the structures are corresponding with an α-helix for the last 16 amino acids residues, whereas the first three N-terminal residues display a higher flexibility. Inspection of the two sets of structures shows a good correlation in the 4–20 region. The nine DG/SA structures with side chains were superimposed over the same region and are shown in Fig. 7. The root-mean-square deviations of the backbone and the side chain atoms positions of the structures generated by DG/SA and SA are displayed in Fig. 8. Averaged RMSD of the backbone atom positions of the helix portion are calculated as 0.77 Å and 0.83 Å, for DG/SA and SA respectively. For the side chains atom positions, the corresponding values are 1.44 Å and 1.49 Å.

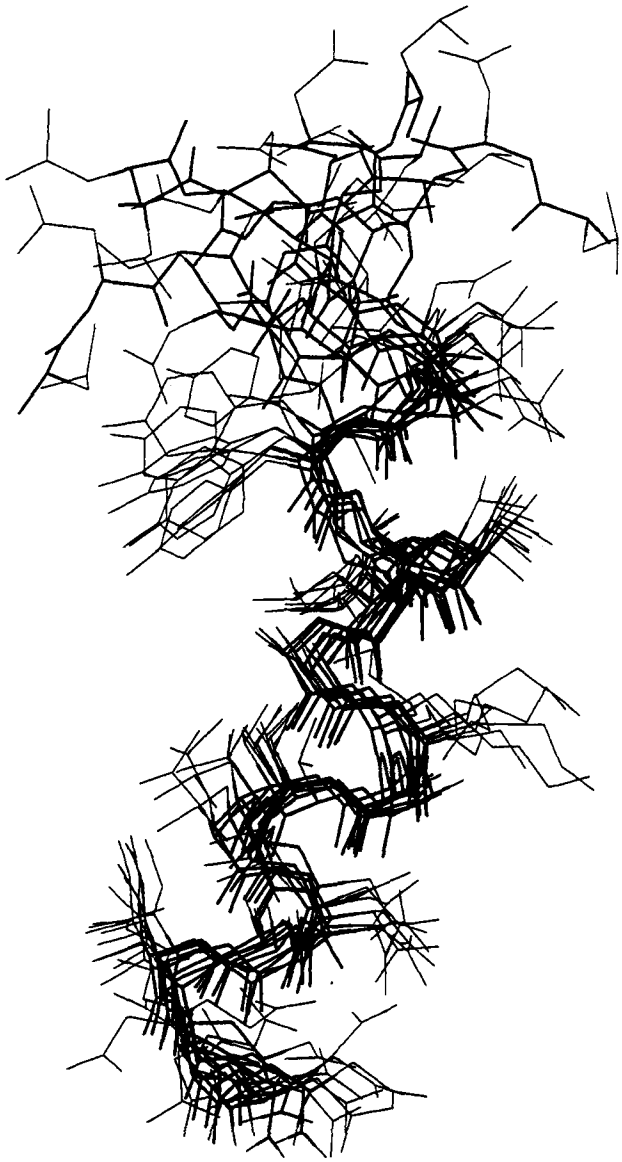

Fig. 7. Superimposition of the 9 accepted structures, showing the side chain atoms, obtained from DG/SA. The structures are positioned as in Fig. 5.

The final refinement with CHARMm full parameter set was designed to check the consistency of the structures generated by the two processes. The relative potential energies of the structures were of reasonable values (averaged value for DG/SA: −202 kcal/mol, and for SA: −194 kcal/mol).

4. Discussion

Trifluoroethanol has been used in order to stabilize peptide conformation [24–30]. More recently, evidences have been described for the good correlation between the

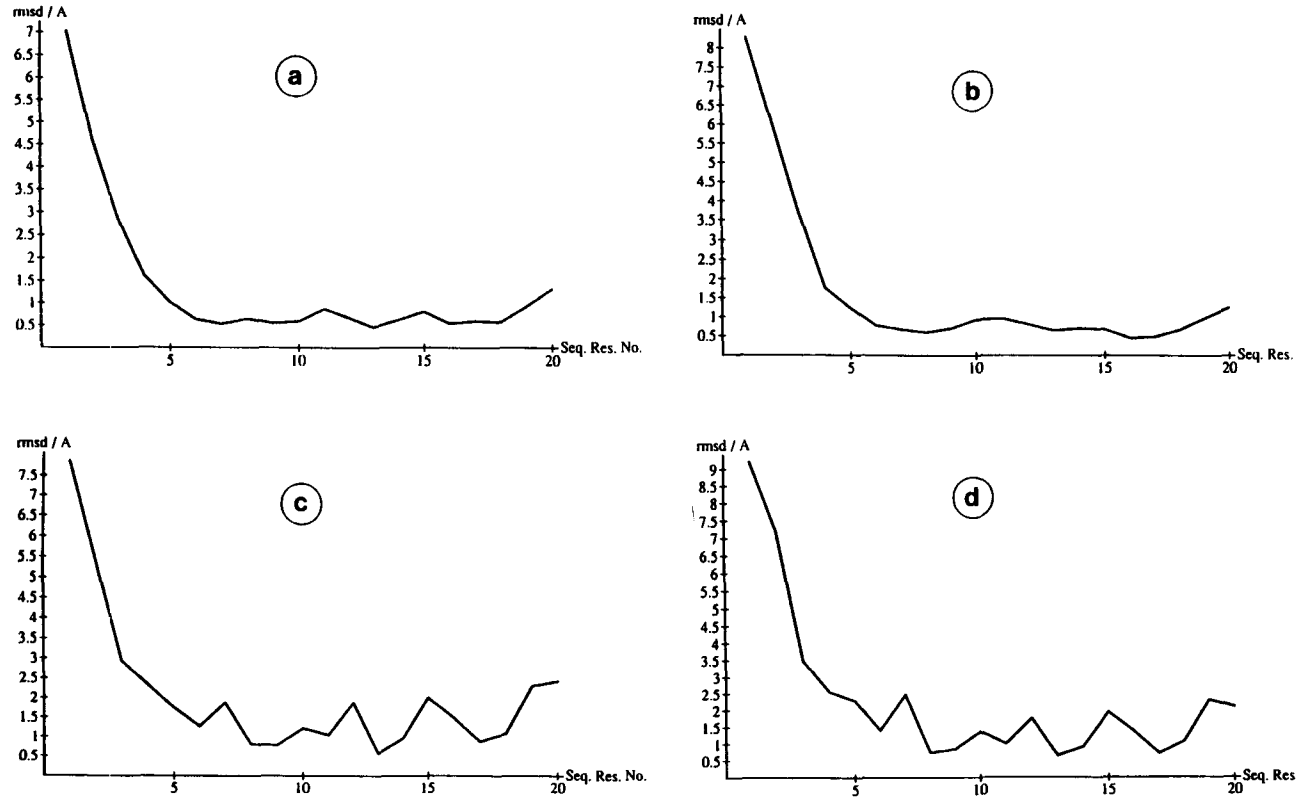

Fig. 8. Averaged root mean square deviations (RMSD) in angstroms of the atom positions of the 9 structures generated by DG/SA (a: backbone; c: side chain) and the 19 structures generated by SA (b: backbone; d: side chain). The structures are best fitted between backbone atoms of residues 4 to 20.

TFE enhancement of peptide α-helicity and the helical tendency of the peptide sequence [31,32]. However, in some cases, the helical enhancement does not correspond to the same conformation in the corresponding region of the whole protein [31]. This difference was mainly associated with the capacity of the tertiary structure of the protein to induce local perturbation in the environment of the peptide [31]. However, in the vast majority of reported studies, there is a good correlation between the TFE-stabilized structure and the structure.within the protein. This is particularly true when the maximum stabilization is reached with a low level of TFE. In this study, the maximum effect of the TFE is slightly below 30% (v/v) (10 mol% in H_2O). This corresponds to one of the lowest values even for an amphipathic peptide, which usually displays the maximum helical character with a relatively low TFE content between 30 and 50% (v/v) [27,33,34]. Furthermore, at 278 K, the immediate aggregation of the peptide occurs with only 10% TFE. This small percentage supports the high propensity of the peptide to adopt α-helix conformation which is enhanced at low temperature.

Nuclear magnetic resonance, with circular dichroism, is a powerful experimental technique to determine the secondary structure of peptides [28,29,32]. NOESY connectivities and $^3J_{NH\text{-}\alpha H}$ coupling constants can be indicative of secondary conformation. Furthermore the three-dimensional solution structure determination, based on NOE distance constraints, is relevant to check the validity of the qualitative NOE information. In this study, we have fully assigned the proton resonances as well as the NOE connectivities of the peptide dissolved in 30% TFE. Based on the presence of numerous d_{NN} $(i, i+1)$ and $d_{\alpha N}$ $(i, i+3)$ cross-peaks, we have proposed the presence of a well-defined α-helix. An helical region encompassing residues 4 to 20 is clearly displayed in the three dimensional structure based on the NMR information. Both methods of calculations, distance geometry or simulated annealing, lead to very similar sets of structures. Clearly, the amphipathic character of the helix can be observed by analysis of the localization of the polar residues. The two charged amino acids (Lys-12 and Asp-16) and the polar residues (Thr-6 and -9, Asn-5 and -20 and Gln-19) are all arranged along one face of the helix. Our data provide experimental evidence for the structure prediction performed with the method of Von Heijne suggesting an amphipathic α-helix conformation for this stretch [8]. However, in the conditions of this study, the first three residues of the synthetic peptide display a large flexibility whereas the predictive approach suggested an helix through the whole fragment. This small discrepancy suggests an imprecision in the predictive method or the presence of constraints imposed, in that segment, by the protein context.

Three main types of helices can be encountered in proteins: membrane spanning helices, membrane surface

seeking helices and globular protein helices [35]. Hydrophobic moment plot analysis and peptide recognition by antibodies raised against membrane bound spiralin (Brenner et al. [36]), suggest that the segment comprising residues 143–162 correspond to an α-helix localized at the surface of a globular domain of spiralin. In this topological model, the anchorage of the protein on the outer face of the plasma membrane is performed by the covalently bound lipidic moieties [5].

Acknowledgements

We thank Drs. P. Guenot and S. Sinbandhit for facilities at the C.R.M.P.O., and Dr B. Gilquin for a careful reading of the manuscript and fruitful comments.

References

[1] Razin, S. (1992) FEMS Microbiol. Lett. 100, 423–432.
[2] Wieslander, Å., Boyer, M.J. and Wróblewski, H. (1992) in Mycoplasmas: Biology and Pathogenesis (Maniloff, J., McElhaney, R.N., Finch, L.R. and Baseman, J.B., eds.), pp. 93–112, American Society for Microbiology, Washington.
[3] Wróblewski, H., Johansson, K.E. and Hjertén, S. (1977) Biochim. Biophys. Acta 465, 275–289.
[4] Wróblewski, H., Robic, D., Thomas, D. and Blanchard, A. (1984) Ann. Inst. Pasteur Microbiol. 135A, 73–82.
[5] Wróblewski, H., Nyström, S., Blanchard, A. and Wieslander, Å. (1989) J. Bacteriol. 171, 5039–5047.
[6] Mouchès, C., Candresse, T., Barosso, G., Saillard, C., Wróblewski, H. and Bové, J.M. (1986) J. Bacteriol. 164, 1094–1099.
[7] Chevalier, C., Saillard, C. and Bové, J.M. (1990) J. Bacteriol. 172, 2693–2703.
[8] Chevalier, C., Saillard, C. and Bové, J.M. (1990) J. Bacteriol. 172, 6090–6097.
[9] Le Hénaff, M., Brenner, C., Fontenelle, C. Delamarche, C. and Wróblewski, H. (1991) C.R. Acad. Sci. Paris, Series III 312, 189–195.
[10] Marion, D. and Wüthrich, K. (1983) Biochem. Biophys. Res. Commun. 113, 967–974.
[11] Plateau, P. and Gueron, M. (1982) J. Am. Chem. Soc. 104, 7310–7311.
[12] Piantini, U., Sørensen, O., and Ernst, R.R. (1984) J. Am. Chem. Soc. 104, 6800–6801.
[13] Rance, M., Sørensen, O.W., Bodenhausen, G., Wagner, G., Ernst, R.R. and Wüthrich, K. (1983) Biochem. Biophys. Res. Commun. 117, 479–485.
[14] Wagner, G. (1983) J. Magn. Reson. 55, 151–156.
[15] Bax, A. and Drobny, G. (1985) J. Magn. Reson. 61, 306–320.
[16] Jeener, J., Meier, B.H., Bachmann, P. and Ernst, R.R. (1979) J. Chem. Phys. 71, 4546–4553.
[17] Cung, M.T., Marraud, M. and Neel, J. (1974) Macromolecules 7, 606–613.
[18] Brunger, A. (1990) XPLOR manual V 3.0, Yale University.
[19] Nilges, M., Clore, G.M. and Gronenborn, A.M. (1988) FEBS Lett. 239, 317–324.
[20] Kuszewski, J., Nilges, M. and Brünger, A. (1992) J. Biomol. NMR 2, 33–56.
[21] Nilges, M., Clore, G.M. and Gronenborn, A.M. (1988) FEBS Lett. 239, 129–136.
[22] Brooks, B.R., Bruccoleri, R.E., Olafson, B.D., States, D.J., Swaminathan, S. and Karplus, M. (1983) J. Comp. Chem. 4, 187–217.
[23] Wüthrich, K. (1986) NMR of Proteins and Nucleic Acids, Wiley, New York.
[24] Nelson, J.W. and Kallenbach, N.R. (1986) Proteins 1, 211–217.
[25] Nelson, J.W. and Kallenbach, N.R. (1989) Biochemistry 28, 5256–5261.
[26] Clore, G.M., Martin, S.R. and Gronenborn, A.M. (1986) J. Mol. Biol. 191, 553–561.
[27] Gooley, P.R. and MacKenzie, N.E. (1988) Biochemistry 27, 4032–4040.
[28] Dyson, H.J., Rance, M., Houghten, R.A., Wright, P.E. and Lerner, R.A. (1988) J. Mol. Biol. 201, 201–217.
[29] Bradley, E.K., Thomason, J.F., Cohen, F.E., Kosen, P.A. and Kuntz I.D. (1990) J. Mol. Biol. 215, 607–622.
[30] Gronenborn, A.M., Boverman, G. and Clore, G.M. (1987) FEBS Lett. 215, 88–94.
[31] Lehrman, S.R., Tuls, J.L. and Lund, M. (1990) Biochemistry 29, 5590–5596.
[32] Sönnichsen, F.D., Van Eyk, J.E., Hodges, R.S. and Sykes B.D. (1992) Biochemistry 31, 8790–8798.
[33] Sanford, D.G., Kanagy, C., Sudmeier, J.L., Furie, B.C., Furie, B. and Bachovchin, W.W. (1991) Biochemistry 30, 9835–9841.
[34] Zagorski, M.G., Norman, D.G., Barrow, C.J., Iwashita, T., Tachibana, K. and Patel, D.J. (1991) Biochemistry 30, 8009–8017.
[35] Eisenberg, D., Weiss, R.M. and Terwilliger, T.C. (1982) Nature 299, 371–374.
[36] Brenner, C., Duclohier, H., Krchňák, V. and Wróblewski, H. (1995) Biochim. Biophys. Acta 1235, 161–168.